Journal of Membrane Science 326 (2009) 137–144

Contents lists available at ScienceDirect

Journal of Membrane Science

journal homepage: www.elsevier.com/locate/memsci

Preparation of stable MCM-48 tubular membranes

M. Pedernera[a], O. de la Iglesia[b], R. Mallada[b,*], Z. Lin[c], J. Rocha[c], J. Coronas[b], J. Santamaría[b]

[a] Planta Piloto de Ingeniería Química – UNS-CONICET, Bahía Blanca, Argentina
[b] Departamento de Ingeniería Química y Tecnologías del Medio Ambiente – Universidad de Zaragoza, España, Spain
[c] Department of Chemistry, University of Aveiro, CICECO, 3810-193 Aveiro, Portugal

ARTICLE INFO

Article history:
Received 27 March 2008
Received in revised form
23 September 2008
Accepted 23 September 2008
Available online 8 October 2008

Keywords:
Mesoporous membranes
MCM-48
Hydrothermal stability
Zeolite
Organic/permanent gas separation

ABSTRACT

Stable mesoporous membranes with a cubic structure, based on the MCM-48 material, were successfully prepared on alumina supports by hydrothermal synthesis, starting from sols having both CTABr and TPAOH structure directing agents. The inclusion of a zeolite (MFI-type) precursor during membrane synthesis led to partial zeolite incorporation into the porous structure, giving rise to a hydrothermally stable membrane. The mean pore diameter of the membrane was 2.5 nm, and permeation experiments confirmed that transport across the membrane was governed by Knudsen diffusion and that there were no pinholes.

The hydrothermal stability of conventionally prepared (MCM-48) and partly zeolitized (MCMZ) powders was studied. Unlike MCM-48 samples (whose surface area sharply decreased after the hydrothermal treatment), the MCMZ surface area remained constant (1031 m^2/g before and 1009 m^2/g after the hydrothermal treatment), indicating a high hydrothermal stability.

MCMZ membranes were tested in the gas phase separation of binary organic (cyclohexane, benzene and n-hexane)/O_2 mixtures. A maximum selectivity of 124 was obtained for the separation of cyclohexane/O_2 mixtures. The selective permeation of the organic compound was made possible by specific interactions between the organic molecules and the mesoporous host materials, and/or by capillary condensation within the membrane pores.

1. Introduction

Within the field of inorganic membranes microporous zeolite membranes are very attractive due to their well-defined pore size and thermal and chemical stability. However, in many membrane separation applications the zeolite pore size is too small to allow the passage of the target molecules, and wider pore materials are needed, such as silica, zirconia, titania prepared by the sol–gel method. While this broadens the pore size to the mesoporous range, membranes made of these materials often present wide pore size distributions that make it difficult to achieve the levels of selectivity that are attainable with zeolite membranes. As a consequence, the preparation of ordered mesoporous membranes, with a narrow pore size distribution becomes highly desirable for applications including membrane separations, chemical sensors and heterogeneous catalysis [1].

In 1992 Mobil Oil Corporation published the synthesis of a new group of mesoporous materials, designated M41S [2,3] with uniform pore structures of hexagonal (MCM-41) and cubic (MCM-48) arrangements. These materials are characterized by narrow pore size distributions, tunable from 2 to 10 nm, and large surface areas (>1000 m^2/g). However, these materials suffer from a relative lack of hydrothermal stability, mainly due to the amorphous character of their walls, prompting extensive efforts to increase material stability by introducing changes in the synthesis procedure or by post-synthetic treatments. Attaining hydrothermal stability of mesostructured materials is very important in many applications where water is involved, such as ion exchange and liquid phase separations, and also in high temperature processes, such as catalytic reactions (e.g. steam reforming) or gas separations (e.g. CO_2 removal), where the presence of steam cannot be avoided.

Perhaps, the most promising techniques to increase hydrothermal stability involve the incorporation of zeolite structures into the walls of mesoporous silica, thus combining the high stability of zeolites and the larger pores of M41S materials.

In recent years, a number of studies have attempted the incorporation of zeolites into M41S, mainly in the highly ordered hexagonal structure [4–9], while the synthesis of hydrothermal stable mesoporous materials with cubic structures, like MCM-48, has received less attention. However, structures with three-dimensionally accessible pores are in principle more adequate not

* Corresponding author. Tel.: +34 976762392; fax: +34 976761879.
E-mail address: rmallada@unizar.es (R. Mallada).

0376-7388/$ – see front matter © 2008 Elsevier B.V. All rights reserved.
doi:10.1016/j.memsci.2008.09.050

only for applications in adsorption and catalysis, but especially in membrane separations. Among the efforts in this direction, Prokešová et al. [10,11] obtained micro/mesoporous composites prepared via simultaneous hydrothermal treatment of a MCM-48 precursor solution and a colloidal solution containing amorphous zeolite seeds. Li et al. [12] used a similar method, avoiding a heating step in the precursor preparation process. They reported a simple one-step hydrothermal synthesis procedure to prepare stable mesoporous materials with a highly ordered cubic structure that contains primary zeolite building units in the walls of the material. Xia and Mokaya prepared a MCM-48 assembled with ZSM-5 seeds [13,14] as well as Beta zeolite/MCM-48 composites [14]. These authors studied the hydrothermal stability and acidity of MCM-48 mesoporous aluminosilicas assembled from ZSM-5 and Beta zeolite seeds, and of Al-MCM-48 prepared either by a direct synthesis method or by a post-synthesis grafting. They found that zeolite/MCM-48 composites presented the highest hydrothermal stability and acidity, and attributed it to the presence of zeolite-like building units in the framework of MCM-48.

All of the above works concerned zeolite/MCM-48 composites as powders. However, as explained above, there is considerable interest in the formation of mesoporous films with controlled pore sizes for permeation applications. Some works have addressed the preparation of low-thickness films of mesoporous MCM-41 on dense substrates [15–18]; although it is clear that this type of substrates do not allow permeation, these investigations provided useful insight into the mechanisms of formation and the arrangement of the porous channels in the film. In general, the silica films described in these works possess one-dimensional pores oriented parallel to the surface of the substrate, which do not allow an easy transport into or through the film. Also, a few works on film formation on porous supports have already appeared in the literature. Nishiyama et al. [19] have synthesized MCM-48 membranes and silylated MCM-48 membranes on flat porous support. The silylated MCM-48 and MCM-48 membranes were used to separate ethanol from an ethanol/water mixture [20]. The authors showed that synthesized silylated MCM-48 membranes were more effective for the separation of organic/water mixtures because of their narrow pore size distribution and the hydrophobicity of the silylated MCM-48 membranes.

McCool et al. [21] fabricated cubic-structure mesoporous membranes by hydrothermal synthesis and sol dip-coating on the surface and/or within the pores of α-alumina support disks. The authors compared the gas permeation through both types of membranes and found that, while Knudsen permeation prevailed on both membranes, the permeation through the hydrothermally prepared membranes was lower due to a larger membrane thickness and to the penetration of the synthesis gel within the support pores, giving rise to partial pore plugging that increased transport resistance. In a previous work of our laboratory [22] we reported on the preparation and characterization of MCM-48 membranes on tubular supports, which were considered as more adequate for industrial processes on account of their high area to volume ratio and their easier scale-up. It was shown that these membranes were able to separate with good selectivity organic compounds from non-adsorbable gases. Depending on the operating conditions, the separation mechanism ranged from specific interactions between the membrane material and the permeating molecules to capillary condensation within the MCM-48 mesopores.

Recently, Kumar et al. [23] studied the effect of surfactant removal either by calcination or solvent extraction on MCM-48 membranes. As also observed in our previous investigation [22], the method of surfactant removal played a key role on the characteristics of the membranes prepared; while calcination was more efficient in removing the surfactant, extraction preserved better the integrity of the MCM-48 films, resulting in membranes of a higher quality.

In spite of the good results obtained in the few works carried out with MCM-48 membranes, the structural stability of membranes composed of M41S materials remains a serious concern, especially in the presence of steam-containing atmospheres. As explained above, with powder samples this problem has been addressed successfully through the incorporation of sufficient zeolite material to provide stability, while preserving mostly unaltered the bulk of the mesoporous structure. Following this approach, in this work, we have prepared stable MCM-48 membranes, within the pores of the alumina support, and powders by means of partial zeolitization (MFI-type zeolite) of the walls of the porous structure using a zeolite-gel precursor during membrane synthesis. The membranes were prepared on different tubular porous alumina supports by hydrothermal synthesis, then characterized by a variety of techniques and tested in the gas phase separation of mixtures containing organic compounds.

2. Experimental

2.1. Synthesis of the membranes

The membranes were prepared on tubular asymmetric supports (Inocermic) of 7 mm I.D., 10 mm O.D. The γ-Al_2O_3 separation layer on these α-Al_2O_3 supports had a pore diameter of either 5 or 60 nm, and was deployed on top of a macroporous support with pores of 1900 nm. In order to delimit the permeation zone, the supports were subjected to enameling at both ends, defining a permeation length of approximately 5 cm.

For the preparation of the membranes one of the synthesis gel compositions given by Li et al. [12], was used, as it allowed single-step preparation of stable MCM-48 powders by introducing zeolite primary building units into the walls of the material. Except for the composition of the precursor gel, the preparation procedure was similar to that reported in our previous work [22]. The precursor gel used in the present work had the following molar composition: 100 SiO_2:10 Na_2O:16,600 H_2O:12 CTABr:0.5 Al_2O_3:16 TPAOH. CTABr and TPAOH stand, respectively, for cetyltrimethylammonium bromide and tetrapropylammonium hydroxide. In a typical synthesis, TPAOH and NaOH were added under stirring to an aqueous solution of $Al_2(SO_4)_3$ 18 H_2O and TEOS. Afterwards, the solution was aged for 20 h at room temperature and then added to an aqueous solution of CTABr under vigorous stirring. The pores of the support were filled with synthesis gel by applying vacuum to the membrane inner side. The support was then introduced in a Teflon-lined autoclave, immersed into synthesis gel, and subjected to hydrothermal treatment in horizontal (rotating) position, for 48 h at 423 K. The synthesis formed the membrane inside the support pores and also produced powdered material, which was collected at the bottom of the autoclave after synthesis and used for later analysis. The resulting powder and membrane were washed with distilled water and dried at room temperature overnight.

The synthesis procedure was repeated until a N_2-impermeable (because of the presence of the organic structure agents in the micro and mesopores) membrane was obtained. The removal of the surfactant was then carried out either by calcination, or by solvent extraction. A two-step procedure was adopted to conduct the calcinations. First the sample was heated under nitrogen atmosphere up to 813 K at a heating rate of 2 K/min, and then maintained at this temperature under flowing air for 6 h. In both steps of the calcination procedure the flux of gas was 200N mL/min. For chemical

extraction a solution containing EtOH and HCl, 4.5 g of HCl solution (37%) and 125 mL of EtOH per each 0.5 g of solid material to be extracted, was used at 328 K for 8 h under reflux. The stable, zeolite-containing materials prepared in this work will be designated as MCMZ-M (membranes) and MCMZ-P (powders) either calcined (MCMZ-PC) or extracted (MCMZ-PE). To compare with the stability of the MCMZ material, two different MCM-48 powders were prepared. One sample (MCM-P1) was prepared using the gel previously employed on the preparation of MCM-48 membranes, (1 SiO_2:61.44 H_2O:0.62 CTMACl:0.5 NaOH) with CTMACl as surfactant; the synthesis was carried out for 48 h at 383 K [24]. The other sample (MCM-P2) containing CTMABr, as in the case of the MCMPZ, was synthesized during 96 h at 373 K in an autoclave using a gel with the following molar composition: 1.4 SiO_2:1 CTABr:0.35 Na_2O:5 EtOH:140 H_2O [25].

2.2. Characterization

The structure of the membranes and powders prepared was characterized by X-ray diffraction (XRD) with Cu Kα radiation on Philips X'pert MPD. The BET surface areas and pore size distributions of the powder were obtained by nitrogen adsorption measurements with a Micromeritics ASAP 2020. The morphology of the membranes was characterized by scanning electron microscopy (SEM), in a JEOL JSM-6400 instrument operating at 20 kV, equipped with a eXL-10, Link analytical system for EDX analysis.

The quality of the membranes was determined by N_2 permeance measurements, and by permporometry. In this technique, the permeation flux of a non-condensable gas was monitored under conditions where the capillary condensation of water or other organic vapours blocks the pores of a given size. This method was employed to measure the pore size distribution of the membranes.

2.3. Separation experiments

The membranes were tested in the separation of cyclohexane/oxygen mixtures, used as a model for the separation of adsorbable/non-adsorbable components. The gas mixture was fed at a rate of 150 mL/min into the tube side of the membrane (retentate) and an inert sweep gas (He, 100 mL/min) was used on the permeate side. The feed mixture (around 10% cyclohexane) was obtained by bubbling an O_2 stream through a saturator that contained the organic compound. Since this composition is within the flammability range for cyclohexane/air mixtures, exhaustive care was taken to avoid any possible ignition source in the path of the mixture. The composition of the feed entering the separation module was accurately established by on-line gas chromatography (HP 5890 Series II equipped with TCD and FID detectors). The experiments were carried out at room temperature, with atmospheric pressure (101 kPa) on both sides of the membrane. When the steady state was reached, samples at the exit of both the tube and the shell side were analyzed by on-line gas chromatography.

The permeation fluxes and the separation selectivity were obtained as follows:

$$S\left(\frac{\text{organic}}{O_2}\right) = \frac{P_{\text{organic}}}{P_{O_2}}$$

$$P_i = \frac{F_p y_{i,p}}{S_p \Delta P_{\log,i}}$$

where S is the selectivity, P_i the permeance of organic component i, y_{ip} the molar fraction of component on the permeate side, S_p the permeable membrane area, ΔP the log mean partial pressure drop and F_p the molar flow on the permeate side.

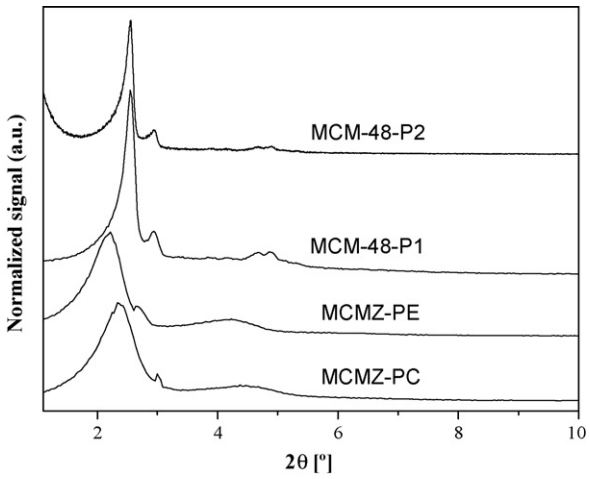

Fig. 1. Diffraction patterns of the synthesized powders: MCMZ-PC, MCMZ-PE, MCM-P1 and MCM-P2.

3. Results

3.1. Characterization of powders

The XRD patterns corresponding to the different powders prepared are presented in Fig. 1. The diffraction peaks of the samples match well the characteristic 3D cubic MCM-48 structure [3]. No diffraction peaks were observed in the region of higher angles for any of the powders tested, including the MCMZ-PC and MCMZ-PE samples, suggesting that the aluminosilicate precursors are in the form of zeolite primary building units, in agreement with the results of Li et al. [12]. In the case of the MCMZ-PC and MCMZ-PE samples all the peaks were still present after removal of the surfactant, though a displacement to higher values of 2θ was detected for the calcined sample. This indicates a decrease in the "d" space of the structure, which could be attributed to shrinkage during calcination. It is worth noting that the 2θ values for the main peaks are lower for zeolitized samples MCMZ-PC and -PE (2.35 and 2.20, respectively) than for as-made samples MCM-48-P1 and -P2 (2.54 and 2.55, respectively). This observation would be consistent with thicker walls for the zeolitied materials, and hence would translate into more stable materials, as will be shown next.

The nitrogen adsorption–desorption isotherms for the calcined, MCMZ-PC (Fig. 2a), and extracted, MCMZ-PE (not shown), samples correspond to a typical type IV isotherm confirming the existence of a mesoporous structure. Table 1 summarizes the parameters obtained from the N_2 adsorption branch using the Barrett–Joyner–Halenda (BJH) and BET methods. Both the calcined and the extracted samples exhibited high surface area and narrow pore size distributions with average pore size values of 3.1 and 2.4 nm, respectively.

The calculated pore volume and the mean pore size were smaller for the extracted sample, suggesting that part of the template was still inside the pore structure. Furthermore in this sample almost all the pore volume corresponds to mesopores, which agrees with the fact that the template is more difficult to extract from the micropores. In spite of this lower efficiency, extraction is still the preferred method for template removal when membrane preparation (rather than powder) is concerned, as membrane integrity is better preserved [18].

The hydrothermal stability of the MCM-P1, MCM-P2 and MCMZ-PC powder samples was assessed from the evolution of surface area measured by N_2 adsorption after exposure to a steam-containing atmosphere. Thus, after template removal (in this case using calci-

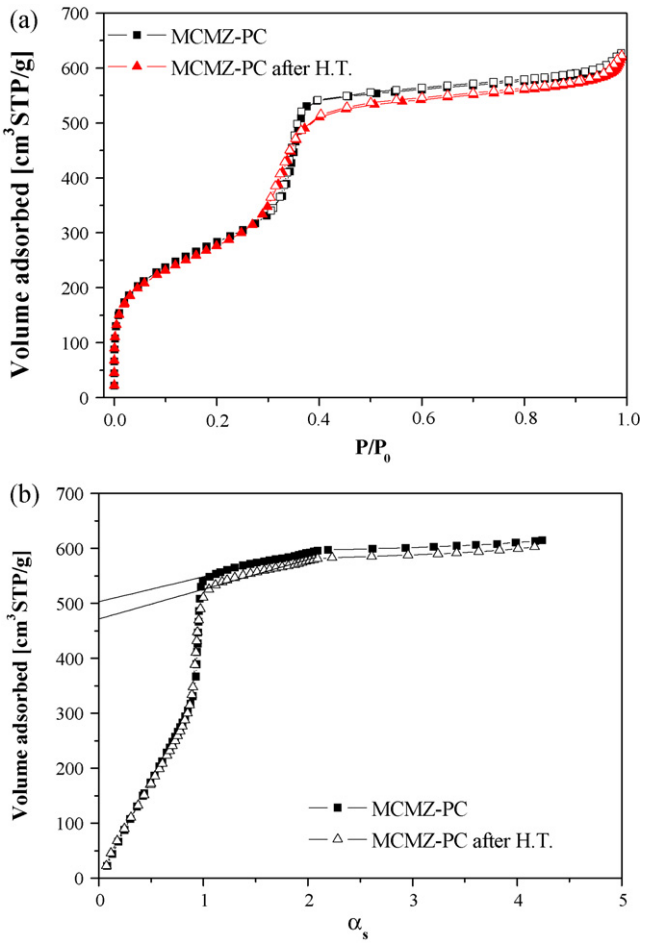

Fig. 2. (a) Nitrogen adsorption–desorption isotherms and (b) α_s-plot for MCMZ-PC sample before and after hydrothermal treatment.

Table 1
Parameters obtained from nitrogen adsorption isotherms on MCMZ powders.

Parameter	MCMZ-PE	MCMZ-PC	MCMZ-PC after HT
BET specific surface area (m^2/g)	1022	1031	1009
Pore volume (cm^3/g)	0.88	1.03	1.01
Average pore diameter (nm)	2.4	3.1	3.1
Mesopore volume (cm^3/g)	0.75	0.78	0.72

nation), the samples were autoclaved under steam at 383 K for 24 h. The BET surface areas measured before and after this hydrothermal treatment of the MCM-P1 powder (Table 2) were 582 and 90 m^2/g, respectively. In the case of MCM-P2 with an initial higher specific surface area of 1225 m^2/g, there was a 65% decrease in surface area after the hydrothermal treatment, in agreement with the results observed by Li et al. [12]. The loss of over 60% of the surface area of the MCM-48 samples in a 24-h treatment indicates a collapse of its porous structure. On the other hand, the surface area of the

Table 2
BET surface areas of MCM-48 (MCM) and partly zeolitized (MCMZ) powder samples before and after hydrothermal treatment.

Sample	BET area (m^2/g)	
	Before	After
MCM-P1	582	90
MCM-P2	1225	425
MCMZ-PC	1031	1009

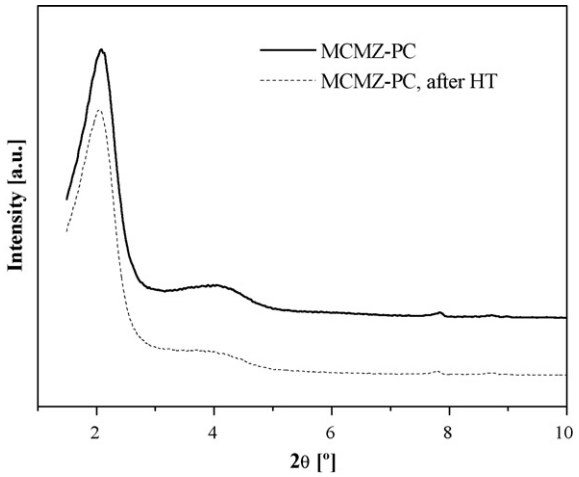

Fig. 3. Diffraction patterns of MCMZ-PC before and after hydrothermal treatment.

MCMZ-PC sample remained nearly constant after the hydrothermal treatment, with a decrease of only 2%, see Table 1.

The α_s-plot and *t*-plot methods have been used to analyze the micro and mesoporosity of these composite materials [5,6,11]. Both methods give rise to similar information, distinguishing the adsorbed volume that corresponds to micropores and mesopores. Fig. 2a shows the N_2 isotherm, where the sharp increase observed at around $P/P_0 = 0.3$, corresponds to the narrow pore size distribution (3.1 nm) of the mesoporous material MCMZ. The structure of this sample still remains after the hydrothermal treatment, as shown by the diffraction patterns presented in Fig. 3. In order to assess whether new micropores have been created during the hydrothermal treatment, the α_s-plot analysis has been carried out [11] for the untreated and hydrothermally treated samples (Fig. 2b). The back-extrapolation to the *Y*-axis of the linear part of the α_s-plot, at α_s values above those corresponding to the volume filling of mesopores (around $P/P_0 = 0.3–0.4$, $\alpha_s = 0.9–1$), yields the mesopore volume V_{ME}, which is similar in both cases, although it could be argued that a small decrease is observed for the hydrotreated sample. In addition, the first linear part of the α_s-plot corresponding to $P/P_0 = 0.05–0.3$ ($\alpha_s = 0.6–0.9$) is attributed to the sorption of nitrogen on the micropores, and on the surface of the mesopores, with the intercept of this section with the *Y*-axis of this line giving the micropore volume, V_{MI}. It can be observed in Fig. 2b that in both samples this intercept corresponds to zero, indicating that the contribution of the zeolite micropores to the total pore volume is negligible. In spite of this, the presence of zeolite can be clearly detected, as will be shown below.

3.2. Characterization of membranes

The prepared membranes, synthesis conditions and N_2-permeances are listed in Table 3. Fig. 4a shows the XRD diagram, low angle region, corresponding to the external surface of the MCMZ-M5 membrane. The intensity of the peaks was lower than that observed with the powders because the combination of a curved membrane surface and XRD measurements at low angle only leaves a small amount of mesoporous material on the X-ray pathway. In spite of this, it can be seen that the XRD of Fig. 4a is compatible with the existence of an ordered structure. The diffraction pattern of the external surface of the membrane in the high angle region is presented in Fig. 4b, the peaks marked with a star corresponding to the alumina support. A small but clearly noticeable contribution of the MFI structure, (main peaks in the regions at 8–9° and 23°),

Table 3
Some relevant characteristics of the synthesized membranes.

Membrane	Support	Surfactant removal	Gain (mg/g)	N_2 permeance (mol/(m^2 s Pa))	% Knudsen
MCMZ-M1[a]	γ-60	–	5.6[b]	2.38×10^{-6}[b]	–
MCMZ-M2	γ-60	–	5.8[b]	1.41×10^{-6}[b]	–
MCMZ-M3	γ-5	Calcination	2.2	3.68×10^{-6}	77.0
MCMZ-M4	γ-5	Calcination	2.6	3.14×10^{-6}	73.4
MCMZ-M5	γ-5	Extraction	3.3	6.65×10^{-9}	87.6
MCMZ-M6	γ-5	Extraction	3.8	5.78×10^{-9}	92.3

[a] Two syntheses.
[b] Without surfactant removal.

can be distinguished, indicating that some crystals of zeolite have been grown up to a size detectable by XRD. These results are in accordance with the SEM observations that will be presented in the following section.

Fig. 5 shows different SEM micrographs and the corresponding EDX analysis of MCMZ-M5 membrane, synthesized on a 5 nm support. In Fig. 5a a closer view of the external surface of the membrane is presented where some small units, around 100–500 nm are observed, probably corresponding to scattered zeolite crystals in accordance to the XRD analysis. Chemical (EDX) analysis in the inner part of the membrane (not shown), revealed 8.1 wt.% of Si. In the external part of the membrane the deposits of MCMZ material can be readily identified in the voids between the α-Al_2O_3 grains of the support. The EDX analysis of the point marked in Fig. 5b), reveals a 25 wt.% of Si. The MCMZ deposits filling the support pores actually constitute the membrane, forming a mesoporous barrier with a narrow pore size distribution (around 2.5 nm) as measured by permporometry. This constitutes a so-called type-A membrane [26], where the membrane material is deposited inside the support pores, and it is able to separate successfully organic/O_2 mixtures, as it will be demonstrated below.

In Table 3 the % of Knudsen contribution to the permeation flux is also reported as an indication of the continuity of the mesoporous barrier created during synthesis. This parameter was obtained after the measurement of N_2 permeance at different values of pressure drop across the membrane (from 2.2 to 5 bar). For weakly or non-interacting gases (such as N_2), the permeance through a porous membrane can be expressed as [27]

$$F = \alpha + \beta P_{av}$$

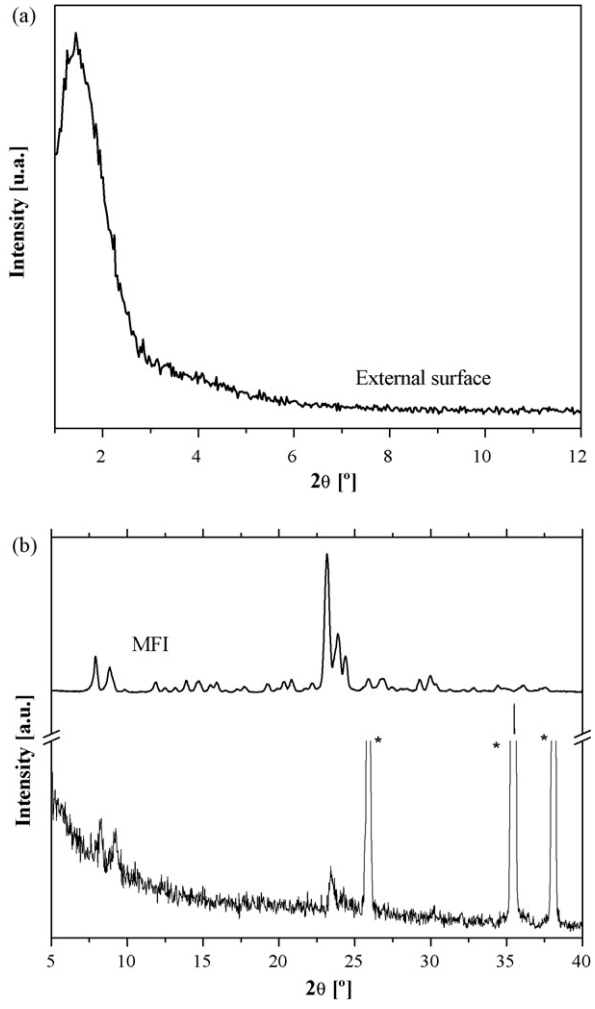

Fig. 4. Diffraction patterns of MCMZ-M5 membrane after calcination. (a) Low angle and (b) high angle.

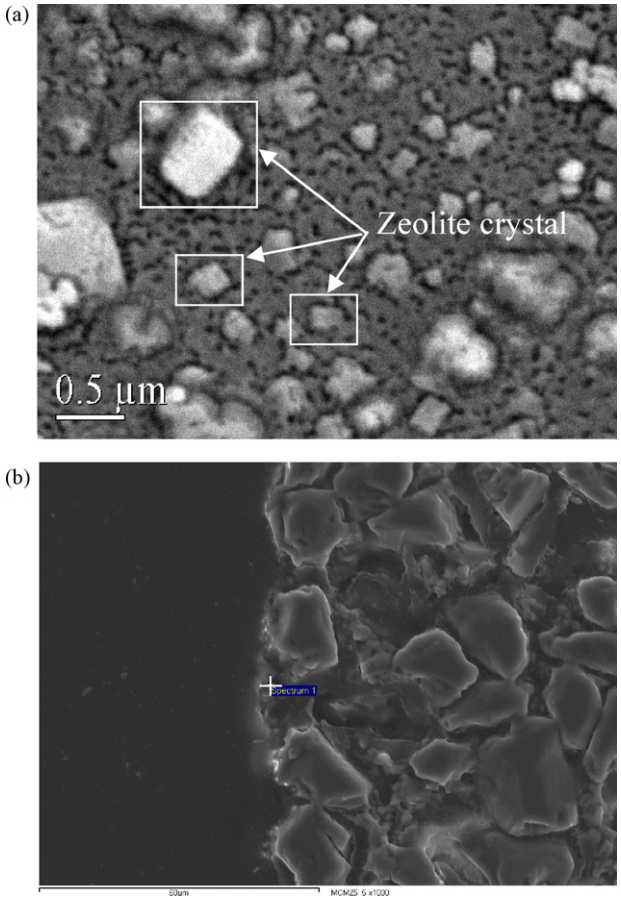

Fig. 5. SEM micrographs of MCMZ-M5 membrane. (a) Top view external surface and (b) cross section external.

where F is the permeation flux per unit time, area and pressure difference (mole/m^2 s bar), P_{av} is the average pressure across the membrane (bar), and α and β indicate the Knudsen and laminar contributions to the permeation flux, respectively. From these two values the percentage contribution of the Knudsen flow to the total flow ($100\alpha/(\alpha+\beta)$) can be obtained, and is given in Table 3 for each of the membranes prepared. Since viscous flow is related to the presence of relatively large inter-crystalline defects, a low value of the viscous contribution (a high value of the % Knudsen) can be taken as a reliable indication of membrane quality. It could be observed that the highest quality membranes were obtained using solvent extraction as the method for surfactant removal, where Knudsen contributions to the permeation flux are around 90%. In contrast, this value drops to less than 80% for calcined membranes, probably reflecting the appearance of cracks in the MCMZ deposits due to thermal stress during calcination. This agrees with the results obtained in our previous work concerning the preparation of MCM-48 membranes [23], and the work recently presented by Kumar et al. [22].

To assess the influence of the hydrothermal treatment on the permeation properties of the membranes, a supplementary experiment was carried out in which the permeance and the Knudsen contribution were compared for the same membrane before and after the same hydrothermal treatment used for the powders. To this end, a MCM-48 membrane with a Knudsen contribution of 71.80% (chosen to be representative of calcined membranes, see Table 3) was used. After 24 h under steam at 383 K no noticeable increase of flux was observed, and the Knudsen contribution was essentially the same (71.05%), indicating that the mechanical integrity of the membrane was retained after the hydrothermal treatment.

As shown in Table 3, those membranes prepared on supports with smaller pore diameter (5 nm) showed lower N_2 permeances, suggesting a higher membrane quality. Using a 60 nm pore diameter support we did not obtain an N_2 impermeable membrane prior to surfactant removal, even if the synthesis procedure was repeated (membrane MCMZ-M1 in Table 3). Although it is unlikely that the entire gamma alumina separation layer survives the harsh, high pH synthesis conditions used, it has influence on the distribution of the MCMZ precursors before synthesis. Thus, since vacuum was applied to the inner membrane side to introduce the synthesis gel into the membrane pores, the flow of the gel was from the outside to the inner side, where the separation layer is located. Hence, a separation layer with a smaller pore diameter was more efficient at retaining the gel.

Permporometry is a non-destructive characterization technique that evaluates the sizes of the pores in a membrane that are available for permeation. It is based on the capillary condensation of a vapour, which has been water in our case. When vapour condenses inside the pores of the membrane, it prevents the permeation of uncondensable gases (N_2 in this case) through the blocked pores. Capillary condensation occurs at different partial pressures that are related to the pore radius by the Kelvin equation. Fig. 6 displays the dimensionless N_2 permeance (i.e. N_2 permeance when using dry nitrogen divided by the N_2 permeance when capillary condensation occurs at a certain vapour partial pressure) vs. the Kelvin diameter, for a 5 nm γ-Al_2O_3 support and MCMZ-M5 membrane.

The mean pore diameter is defined [28] as the diameter that corresponds to a dimensionless permeance of 50%. As expected, the mean pore diameter found for the support corresponds to the one given by the supplier, 5 nm. In the case of MCMZ-M5 membrane, the mean pore diameter was 2.5 nm matching satisfactorily the N_2 adsorption data presented for the MCMZ-PE powder (2.4 nm).

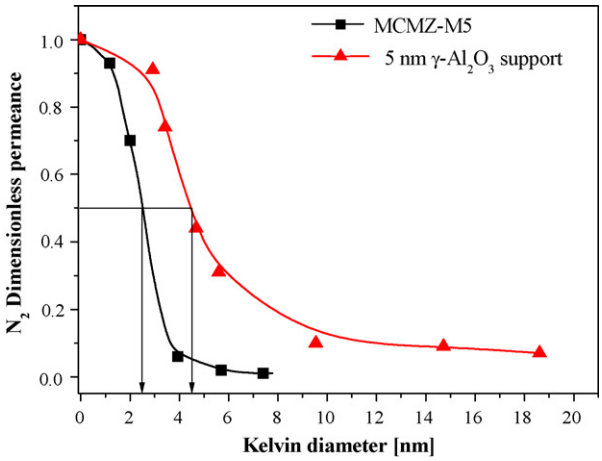

Fig. 6. Dimensionless permeance as a function of Kelvin diameter for MCMZ-M5 membrane and 5 nm γ-Al_2O_3 support.

3.3. Separation of organic/oxygen mixtures

The MCMZ-M membranes were tested in the gas phase separation of binary mixtures containing an organic compound (cyclohexane, n-hexane or benzene) and a permanent gas (O_2). The experiments were carried out at room temperature, with molar concentrations of the organic component in the feed in the 6–14% (vol.) range, and with feed and sweep gas flow rates of 150 and 100N mL/min respectively.

Cyclohexane permeances and cyclohexane/O_2 separation selectivities for the membranes prepared on supports of 5 nm pore diameter are summarized in Table 4 at concentrations of the organic vapour around 10% (vol.) (obtained by flowing an O_2 stream through a bubbler that contained the organic compound at a controlled temperature). The best separation results were obtained when the surfactant was eliminated through solvent extraction (MCMZ-M5 and MCMZ-M6). These membranes showed the highest percentage of Knudsen contribution and the lowest N_2 permeance (Table 3). Cyclohexane/O_2 separation selectivities as high as 124 were obtained, similar to those achieved with MCM-48 membranes [23].

Membranes MCMZ-M5 and MCMZ-M6 were also tested in the gas phase separation of mixtures of benzene/O_2 and n-hexane/O_2. These experiments were carried out with feed concentrations around 6% and 14% (vol.) for benzene and n-hexane, respectively, under the same conditions applied to the separation of cyclohexane/O_2 mixtures.

Fig. 7 shows the organic/O_2 separation selectivity for the three compounds on two different MCMZ membranes. The highest selectivity was obtained with cyclohexane followed by benzene and then by n-hexane, despite its lowest concentration. These results agree with those obtained with MCM-48 membranes and corroborate the conclusions drawn in our previous paper [22], i.e., that the separation selectivity obtained was the result of the cooperative effects

Table 4
Selectivity of cyclohexane/O_2 separations and cyclohexane permeances.

Membrane	Selectivity	Permeance of cyclohexane (mol/(m^2 s Pa))
MCMZ-M3	3.5	8.66×10^{-7}
MCMZ-M4	2.5	5.68×10^{-7}
MCMZ-M5	119	5.04×10^{-7}
MCMZ-M6	124	4.94×10^{-7}

Room temperature, feed flow: 150N mL/min; sweep flow: 100N mL/min. Feed cyclohexane concentration = 10%.

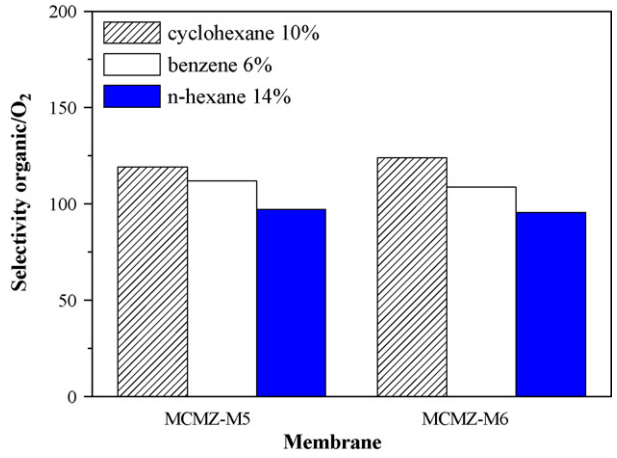

Fig. 7. Selectivity organic/O_2 for MCMZ-M5 and -M6 membranes room temperature, feed flow: 150N mL/min; sweep flow: 100N mL/min. Organic concentrations: cyclohexane 10%, benzene 6% and n-hexane 14%.

of capillary condensation in the pores of the membrane (when allowed by the operating conditions) and of specific interactions between the organic compounds and the mesoporous material. The latter effect becomes more evident when Kelvin diameters are taken into account (Fig. 8). Under the conditions used, the Kelvin diameter was higher than the mean diameter obtained by permporometry (2.5 nm) for the MCMZ membranes, and therefore capillary condensation is expected to take place. However, the capillary condensation alone cannot explain the selectivity results observed. Indeed, for the 5 nm γ-Al_2O_3 support, where capillary condensation takes place but other interactions are not significant the selectivity obtained, 12, while considerably higher than the Knudsen value is much lower than the corresponding selectivity values of the MCMZ-M membranes, around 100. Also, a direct relationship does not exist between the Kelvin diameters corresponding to the separation conditions of each organic compound and the separation selectivities attained, as can be seen in Fig. 8, where the highest selectivity values are obtained for cyclohexane (highest value of Kelvin diameter under the conditions employed), then for benzene (lowest Kelvin diameter) and finally for n-hexane (intermediate Kelvin diameter). Therefore, the higher pore-blocking capacity of cyclohexane and benzene is due not only to capillary condensation, as already stated, but also to specific interactions that can be related to the adsorption affinity and molecular sizes of the different compounds. The adsorption characteristics of these compounds on MCM-41 were studied by Zhao et al. [29] finding that the activation energies for desorption followed the order cyclohexane ≈ benzene > n-hexane. This order agrees well with the results obtained, if we assume a similar affinity of these compounds on MCM-48. Also, n-hexane is not only less voluminous than cyclohexane or benzene, but also can be adsorbed in parallel to the pores. It is therefore expected that cyclohexane and benzene are more effective at blocking the passage of oxygen.

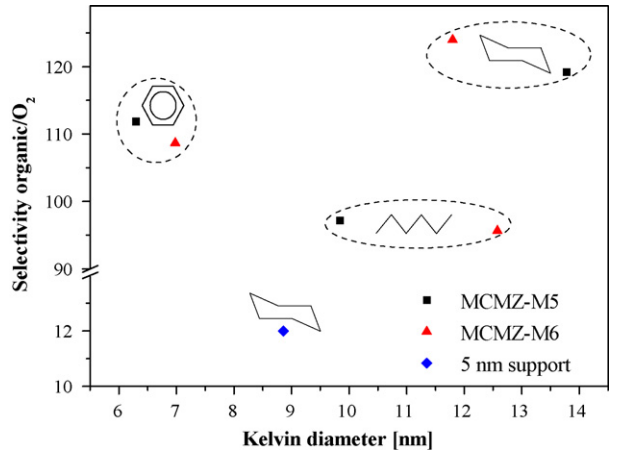

Fig. 8. Kelvin diameters calculated from the separation experiments for MCMZ-M5 and MCMZ-M6 membranes, and for the 5 nm γ-Al_2O_3 support.

4. Conclusions

The synthesis of both mesoporous powders and membranes with zeolite units embedded in the walls was successfully achieved by the procedures described in this work. The materials so obtained were hydrothermally stable, as shown by the comparison of samples MCM-48 and MCMZ where the latter were able to maintain their porous structure after being subjected to hydrothermal treatment, while the former underwent structural collapse. The partly zeolitized membranes are mainly formed inside the support pores. The N_2 permeance and the measurement of the percentage of Knudsen flow indicated that the best quality membranes were those prepared under rotation on 5 nm pore diameter γ-Al_2O_3 supports, and where surfactant was removed by solvent extraction.

The selectivities in the separation of the organic/O_2 mixtures were around 100, following the order: cyclohexane > benzene > n-hexane. The separation is achieved by a cooperative mechanism involving capillary condensation of the organic compound and specific interactions of the organic molecules with the mesoporous material.

Acknowledgements

Financial support from DGA and MEC, both in Spain, is gratefully acknowledged.

References

[1] V.V. Guliants, M.A. Carreon, Y.S. Lin, Ordered mesoporous and macroporous inorganic films and membranes, J. Membr. Sci. 235 (1–2) (2004) 53.
[2] C.T. Kresge, M.E. Leonowicz, W.J. Roth, J.C. Vartulli, J.S. Beck, Ordered mesoporous molecular sieves synthesized by a liquid-crystal template mechanism, Nature 359 (1992) 710.
[3] J.S. Beck, J.C. Vartulli, W.J. Roth, A new family of mesoporous molecular-sieves prepared with liquid-crystal templates, J. Am. Chem. Soc. 114 (1992) 10834.
[4] Y.-S. Ooi, R. Zakaria, A.R. Mohamed, S. Bhatia, Synthesis of composite material MCM-41/Beta and its catalytic performance in waste used palm oil cracking, Appl. Catal. A: Gen. 274 (2004) 15.
[5] S. Wang, T. Dou, Y. Li, Y. Zhang, X. Li, Z. Yan, Synthesis, characterization, and catalytic properties of stable mesoporous molecular sieve MCM-41 prepared form zeolite mordenite, J. Solid State Chem. 177 (2004) 4800.
[6] S. Wang, T. Dou, Y. Li, Y. Zhang, X. Li, Z. Yan, A novel method for the preparation of MOR/MCM-41 composite molecular sieve, Catal. Commun. 6 (2005) 97.
[7] A. Karlsson, M. Stocker, R. Schmidt, Composites of micro- and mesoporous materials: simultaneous synthesis of MFI/MCM-41 like phases by a mixed template approach, Micropor. Mesopor. Mater. 27 (1999) 181.
[8] V. Mavrodinova, M. Popova, V. Valchev, R. Nickolov, Ch. Minchev, Beta zeolite colloidal nanocrystals supported on mesoporous MCM-41, J. Colloid Interf. Sci. 286 (2005) 286.
[9] Z. Zhang, Y. Huan, F.-S. Xiao, S. Qiu, L. Zhu, R. Wang, Y. Yu, Z. Zhang, B. Zou, Y. Wang, H. Sun, D. Zhao, Y. Wei, Mesoporous aluminosilicates with ordered hexagonal structure, strong acidity, and extraordinary hydrothermal stability at high temperatures, J. Am. Chem. Soc. 123 (2001) 5014.
[10] P. Prokešová, S. Mintova, J. Čejka, T. Bein, Preparation of nanosized micro/mesoporous composites via simultaneous synthesis of Beta/MCM-48 phases, Micropor. Mesopor. Mater. 64 (2003) 165.
[11] P. Prokešová-Fojtíková, S. Mintova, J. Čejka, N. Žilková, A. Zukal, Porosity of micro/mesoporous composites, Micropor. Mesopor. Mater. 92 (2006) 154.
[12] Y. Li, J. Shi, H. Chen, Z. Hua, L. Zhang, M. Ruan, J. Yan, D. Yan, One-step synthesis of hydrothermally stable cubic mesoporous aluminosilicates with a novel particle structure, Micropor. Mesopor. Mater. 60 (2003) 51.
[13] Y. Xia, R. Mokaya, On the synthesis and characterization of ZSM-5/MCM-48 aluminosilicate composite materials, J. Mater. Chem. 14 (2004) 863.

[14] Y. Xia, R. Mokaya, Are mesoporous silicas and aluminosilicas assembled from inherently hydrothermally stable? Comparative evaluation of MCM-48 materials assembled from zeolite seeds, J. Mater. Chem. 14 (2004) 3427.
[15] H. Yang, A. Kuperman, N. Coombs, S. Mamiche-Afara, G.A. Ozin, Synthesis of oriented films of mesoporous silica on mica, Nature 379 (1996) 703.
[16] M. Ogawa, A simple sol-gel route for the preparation of silica-surfactant mesostructured materials, Chem. Commun. (1996) 1149.
[17] I.A. Aksay, M. Trau, S. Manne, I. Honna, N. Yao, L. Zhou, P. Fenter, P.M. Eisenberger, S.M. Gruner, Biometric pathways for assembling inorganic thin films, Science 273 (1996) 892.
[18] D. Zhao, P. Yang, N. Melosh, J. Feng, B.F. Chmelka, G.D. Stucky, Continuous mesoporous silica films with highly ordered large pore structures, Adv. Mater. 10 (1998) 1380.
[19] N. Nishiyama, D.H. Park, A. Koide, Y. Egashira, K. Ueyama, A mesoporous silica (MCM-48) membrane: preparation and characterization, J. Membr. Sci. 182 (2001) 235.
[20] D.H. Park, N. Nishiyama, Y. Egashira, K. Ueyama, Separation of organic/water mixtures with silylated MCM-48 silica membranes, Ind. Eng. Chem. Res. 40 (2001) 6105.
[21] B.A. McCool, N. Hill, J. Di Carlo, W.J. DeSisto, Synthesis and characterization of mesoporous silica membranes via dip-coating and hydrothermal deposition techniques, J. Membr. Sci. 218 (2003) 55.
[22] O. de la Iglesia, M. Pedernera, R. Mallada, Z. Lin, J. Rocha, J. Coronas, J. Santamaría, Synthesis and characterization of MCM-48 tubular membranes, J. Membr. Sci. 280 (2006) 867.
[23] P. Kumar, J. Ida, S. Kim, V.V. Guliants, J.Y.S. Lin, Ordered mesoporous membranes: effects of support and surfactant removal conditions on membrane quality, J. Membr. Sci. 279 (2006) 539.
[24] J. Xu, Z. Luan, H. He, W. Zhou, L. Kevan, A reliable synthesis of cubic mesoporous MCM-48 molecular sieve, Chem. Mater. 10 (1998) 3690.
[25] J.M. Kim, S.K. Kim, R. Ryoo, Synthesis of MCM-48 single crystals, Chem. Commun. 2 (1998) 259.
[26] M.P. Bernal, J. Coronas, M. Menéndez, J. Santamaría, On the effect of morphological features on the properties of MFI zeolite membranes, Micropor. Mesopor. Mater. 60 (2003) 99.
[27] Y.S. Lin, A.J. Burggraaf, Preparation and characterization of high-temperature thermally stable alumina composite membrane, J. Am. Ceram. Soc. 74 (1991) 219.
[28] T. Tsuru, T. Hino, T. Yoshioka, M. Asaeda, Permporometry characterization of microporous ceramic membranes, J. Membr. Sci. 186 (2001) 257.
[29] X.S. Zhao, G.Q. Lu, X. Hu, Organophilicity of MCM-41 adsorbents studied by adsorption and temperature-programmed desorption, Colloid Surf. A 179 (2001) 26.